A&A 401, 491–498 (2003)
DOI: 10.1051/0004-6361:20030143
© ESO 2003

Astronomy & Astrophysics

The dark burst 010214 with *BeppoSAX*: Possible variable absorption and jet X–ray emission

C. Guidorzi[1], F. Frontera[1,2], E. Montanari[1,7], L. Amati[2], L. A. Antonelli[3], J. J. M. in 't Zand[4], E. Costa[5], R. Farinelli[1], M. Feroci[5], J. Heise[4], N. Masetti[2], L. Nicastro[6], M. Orlandini[2], E. Palazzi[2], and L. Piro[5]

[1] Dipartimento di Fisica, Università di Ferrara, via Paradiso 12, 44100 Ferrara, Italy
[2] Istituto Astrofisica Spaziale e Fisica Cosmica, Sezione di Bologna, CNR, via Gobetti 101, 40129 Bologna, Italy
[3] Osservatorio Astronomico di Roma, via Frascati 33, Monteporzio 00040, Italy
[4] Space Research Organization in the Netherlands, Sorbonnelaan 2, 3584 CA Utrecht, The Netherlands
[5] Istituto Astrofisica Spaziale e Fisica Cosmica, Sezione di Roma, CNR, via Fosso del Cavaliere, 00133 Roma, Italy
[6] Istituto Astrofisica Spaziale e Fisica Cosmica, Sezione di Palermo, CNR, via U. La Malfa 153, 90146 Palermo, Italy
[7] ITA "I. Calvi", Finale Emilia (MO), Italy

Received 10 October 2002 / Accepted 22 January 2003

Abstract. We report on the prompt and afterglow emission observations of the dark burst GRB010214 with *BeppoSAX*. The prompt emission shows possible evidence of variable absorption from $N_{\rm H} = 3.0^{+5.1}_{-2.0} \times 10^{23}$ cm^{-2} in the first 6 s of the event to a value consistent with the Galactic column density ($N_{\rm H}^{\rm G} = 2.66 \times 10^{20}$ cm^{-2}) in the GRB direction. An X–ray afterglow emission in the 2–10 keV energy band was detected with *BeppoSAX*, but an analogue search at lower wavelengths (optical, IR and radio) was unsuccessful. The X–ray afterglow spectrum is consistent with a power–law with Galactic absorption. The light curve shows a complex decay, if the tail of the prompt emission is assumed as the onset of the afterglow: if the origin of the afterglow is coincident with the GRB onset, a bump before $\sim 3 \times 10^4$ s is inferred, while if the afterglow is assumed to start later, a steepening of the power–law light curve at $t \sim 3 \times 10^4$ s is deduced. We discuss these results in the light of the current models of afterglows and the possible origin of the GRB darkness. Finally, we tentatively derive an estimate of the burst redshift.

Key words. gamma rays: bursts – gamma rays: observations

1. Introduction

The available sample of more than 30 X–ray afterglows of Gamma-Ray Bursts (GRBs) detected with *BeppoSAX* (Frontera 2002; Piro 2002) shows a variety of emission properties that, even if they can be basically accounted for in the context of the fireball model (see, e.g., review by Piran 1999, 2000), shed light on several details of the GRB phenomenon. For example, breaks in the X-ray light curves, inferred by comparing the late afterglow emission with the prompt emission from GRB990510 (Pian et al. 2001) and GRB010222 (In 't Zand et al. 2001), not only confirm the breaks observed in the optical afterglow emission of these GRBs (Stanek et al. 1999, and Harrison et al. 1999, for GRB990510; Masetti et al. 2001a, for GRB010222) but also give support to the fact that the onset of the X–ray afterglows occurs during the tail of the prompt GRB emission (Frontera et al. 2000). Achromatic breaks in the afterglow emission can be an imprint of a relativistic jet when it slows down and spreads laterally (Sari et al. 1999), but can also be, e.g., the consequence of a transition of the relativistic fireball to a non-relativistic regime (NR) in a dense circumburst medium (Dai & Lu 1999). The different relationships expected between the slope of the afterglow light curve and that of the energy spectrum can help to distinguish between the various models and allow to gain information on the circumburst medium properties. In the case of GRB010222, In 't Zand et al. (2001) and Masetti et al. (2001a) find that the NR effect is more consistent with the data. In this respect, some authors suggest that jet effects could not be the unique reason for such breaks (Wei & Lu 2002). The continuum energy spectra of the X–ray afterglows are generally well fit with power–laws. However their interpretation is not unique: they can be either due to synchrotron emission, as in the case of GRB970508 (Galama et al. 1998) or to inverse–Compton emission as in the case of GRB000926 (Harrison et al. 2001). Only broad band spectra, that cover frequency ranges from the radio to X–rays, can provide the handle on the right model. Detection of inverse-Compton emission is a strong hint for the presence of a dense medium around the GRB location.

Send offprint requests to: C. Guidorzi,
e-mail: guidorzi@fe.infn.it

X–ray afterglows have been measured in 86% of the localized GRBs (e.g., Frontera 2002; Piro 2002), but only 50% of the GRBs with X–ray afterglows show optical (OTs) and/or radio transients (RTs). The explanation for the non–detection of OTs is not well established. A possible interpretation of such "dark bursts" in visible light is that they are obscured by dust in their host galaxies (see reviews by Djorgovski 2001 and Pian 2002). This interpretation is likely to be valid when we observe radio transients (RTs) without OTs; in the remaining cases the issue is still open. A possibility is that dark bursts are at very high redshifts ($z \gtrsim 4.5$), as first suggested by Fruchter (1999). The shape of the light curve of the X-ray afterglows can provide a hint on the presence of dense star–forming regions around GRBs: a bump followed by a steeper decay in soft X–rays is predicted for bursts that are heavily obscured in the optical (Mészáros & Gruzinov 2000).

In these respects GRB010214 shows interesting features which we will report and discuss in this paper. As we will see, it showed an X–ray afterglow emission but no positive signal was detected either in the optical or in the radio bands. Thus, it belongs to the class of "dark" bursts.

2. Observations and data analysis

GRB010214 was detected on February 14, 2001, at 08:48:11 UT with the *BeppoSAX* (Boella et al. 1997) Gamma-Ray Burst Monitor (GRBM, 40–700 keV, Frontera et al. 1997), and the Wide Field Camera No. 2 (WFC, 2–28 keV, Jager et al. 1997). The GRB position was promptly estimated with an error circle of radius 3′ (Gandolfi 2001). The BeppoSAX Narrow Field Instruments (NFI) started observing the GRB error box 6.28 hrs after the burst; the observation lasted 1.91 days, with a net exposure time of 83 ks for the MECS and 23 ks for the LECS. A new uncatalogued X–ray source was detected within the WFC error circle in both MECS and LECS at coordinates $\alpha_{2000.0} = 17^{\rm h}40^{\rm m}58^{\rm s}, \delta_{2000.0} = +48°34'37''$ with an error radius of 1′ (Frontera et al. 2001; Guidorzi et al. 2001), showing an apparent decaying flux. Optical/IR/radio counterpart observations of the GRB error box did not find any fading source (see Klose et al.2001a; Zhu & Xue 2001; Hudec et al. 2001; Berger & Frail 2001; Antonelli et al. 2001; Uemura et al. 2001; Gorosabel et al. 2001a, 2001b; Masetti et al. 2001b; Rol et al. 2001a; Cowsik 2001; Henden 2001), in spite of some initial IR (Di Paola et al. 2001) and optical (Rol et al. 2001b; Klose et al. 2001b) claim of afterglow candidate. Among the upper limits reported above, the most constraining ones are shown in Fig. 8.

Data available from GRBM include two 1 s ratemeters in two energy channels (40–700 keV and >100 keV), 128 s count spectra (40–700 keV, 225 channels) and high time resolution data (down to 0.5 ms) in the 40–700 keV energy band. WFCs were operated in normal mode with 31 channels in the 2–28 keV energy band and 0.5 ms time resolution (Jager et al. 1997). The burst direction was offset by 7° with respect to the WFC axis. With this offset, the effective area exposed to the GRB was ≈510 cm^2 in the 40–700 keV band and 72 cm^2 in the 2–28 keV energy band. The background in the WFC and GRBM energy bands was fairly stable during the event. The GRBM background level was estimated by linear interpolation using the 250 s count rate data before and after the burst. The WFC spectra were extracted through the Iterative Removal Of Sources procedure (IROS, e.g. Jager et al. 1997) which implicitly subtracts the contribution of the background and of other point sources in the field of view.

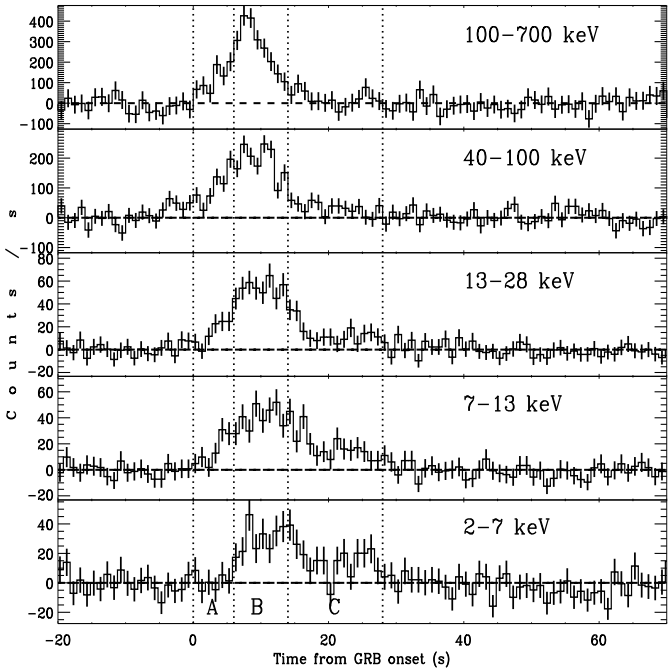

Fig. 1. Light curves of GRB010214 in five energy bands, after background subtraction. The zero abscissa corresponds to 2001 February 14, 08:48:05.1 UT. The three time intervals A, B and C over which the spectral analysis has been performed are indicated with vertical dotted lines.

We performed a joint spectral analysis of the LECS and MECS 2+3 data. The source was apparent in the 2–10 keV energy band, but did not show any statistically significant signal in the 0.1–2.0 keV band covered by the LECS. In 2–10 keV the source was apparent up to 72 ks from the GRB onset. In the last part of the source observation, from 72 to 187 ks, the source was no more visible.

The spectral fitting was performed using the XSPEC package v. 11.0.1 (Arnaud 1996). The elemental abundances are with respect to those by Anders & Ebihara (1982) and the opacities are from Morrison & McCammon (1983). The quoted errors are intended to be at 90% confidence level (cl) for one parameter ($\Delta\chi^2 = 2.7$), except when otherwise specified.

3. Results

3.1. Prompt emission

The GRBM and WFC light curves in different energy bands are shown in Fig. 1. Above 7 keV, the GRB shows a single pulse, which broadens with decreasing energy. A tail after the peak in the WFC energy band is also apparent. In the lowest energy band (2–7 keV), the main pulse shortens and the tail becomes

a secondary peak. The total duration of the burst in the GRBM passband is ∼15 s, while in the low energy X–ray band it is ∼30 s.

The time-averaged 2–700 keV GRB spectrum was derived using the WFC data and the 225 channel GRBM count data. A simple power–law (PL) does not fit ($\chi^2/d.o.f. = 38.5/17$) the data, which are instead well fit ($\chi^2/d.o.f. = 11.7/16$) with a photoelectrically absorbed broken power–law (BKNPL) with photon index $\Gamma_X = 0.86^{+0.13}_{-0.17}$ below the break energy $E_0 = 67^{+20}_{-15}$ keV and $\Gamma_\gamma = 2.4^{+0.3}_{-0.2}$ above E_0 (see Table 1). The fit with a smoothly broken power–law (BL, Band et al. 1993) does not allow the determination of the high energy photon index. By fixing it to the value derived from the BKNPL model, the fit results are reported in Table 1. The $N_{\rm H}$ is consistent with the Galactic value $N_{\rm H}^{\rm G} = 2.66 \times 10^{20}$ cm^{-2} along the GRB direction ($l = 75.3°$, $b = +31.3°$). From the time-averaged GRB spectrum, we derived a GRB 1 s peak flux of $(7.8 \pm 1.3) \times 10^{-7}$ erg cm^{-2} s^{-1} and a 40–700 keV fluence $S_{40-700} = (4.5 \pm 0.8) \times 10^{-6}$ erg cm^{-2} . In the 2–28 keV band the fluence is $S_{2-28} = (7.3 \pm 1.1) \times 10^{-7}$ erg cm^{-2} , with a S_{2-28}/S_{40-700} ratio of about 0.16. For comparison with the BATSE GRBs, the 50–300 keV fluence of GRB010214 is $S_{50-300} = (3.3 \pm 0.7) \times 10^{-6}$ erg cm^{-2} with a hardness ratio $C(100-300)/C(50-100) = 1.2 \pm 0.3$.

The results of the investigation on the spectral evolution of the GRB prompt emission are reported in Table 1 and Fig. 2. The GRB light curve was subdivided in three time intervals A, B and C (see Fig. 1) and the spectrum of each interval derived. The spectrum of the interval A is found to be well fit by a photoelectrically absorbed PL model, with column density $N_{\rm H} = 3.0^{+5.1}_{-2.0} \times 10^{23}$ cm^{-2}, significantly in excess of the Galactic $N_{\rm H}^{\rm G}$. Freezing $N_{\rm H}$ to the Galactic value ($N_{\rm H}^{\rm G}$), the fit is not acceptable ($\chi^2/d.o.f. = 15.8/5$). An alternative to the PL model is the BKNPL model, which fit the data (see Table 1) even assuming a Galactic absorption. However the peak energy $E_{\rm p}$ derived with this model (∼40 keV) contradicts the usual hard-to-soft spectral evolution of GRBs. For this reason, we prefer the PL model, which implies an initial $E_{\rm p} > 700$ keV.

Unlike the A spectrum, the B spectrum cannot be fit with a PL model with either Galactic ($\chi^2/d.o.f. = 18/9$) or higher $N_{\rm H}$ ($\chi^2/d.o.f. = 15.1/8$). It can be fit with either a BKNPL or a BL model with Galactic column density (see Table 1). Finally the C spectrum is mainly constrained by the WFC data, given that we have only upper limits with GRBM. It can be fit by a BKNPL model with Galactic absorption. Freezing the low energy photon index to the value (0.81) found from the fit with a PL with an exponential cutoff, the other parameter values are reported in Table 1.

From the visual inspection of the 1 s light curves (Fig. 1) it is apparent that the pulse peak in the higher energy band leads that at lower energies while the pulse width decreases. This property is not new (Fenimore et al. 1995; Norris et al. 1996). We have evaluated, as a function of energy, both the time lag ΔT of the pulse peak with respect to the 100–700 keV peak time and the pulse $FWHM$ by fitting the pulse time profiles shown in Fig. 1 with a Gaussian plus a polynomial. The results are shown in Fig. 3. Both $FWHM$ and ΔT vs. energy are well fit with a power–law ($\propto E^{-\alpha}$). The best fit index α_{FWHM} is either 0.20 ± 0.10 or 0.28 ± 0.13, depending whether the midpoints or the lower bounds of the energy bands are taken into account, respectively, while the best fit power–law index $\alpha_{\Delta T}$ is 0.55 ± 0.17. The width of the main pulse in the energy channel below 7 keV (see Fig. 1) shortens instead of broadening, but a secondary pulse rises. Only the sum of their $FWHM$, evaluated by rebinning the 2–7 keV light curve at 5 s, is consistent with the power–law slope evaluated at higher energies (see Fig. 3).

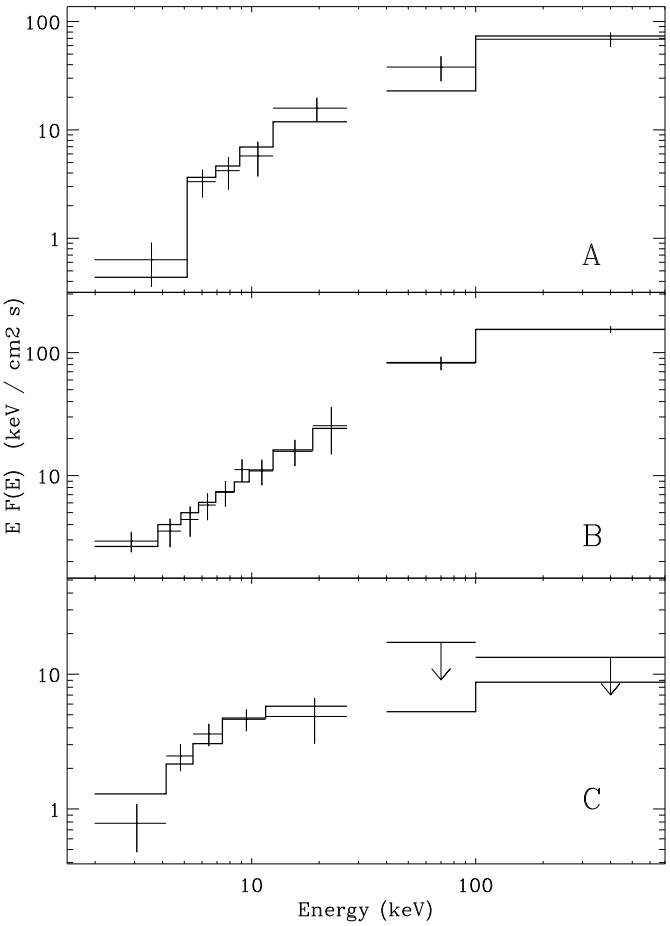

Fig. 2. $EF(E)$ spectrum of the prompt emission in the A, B, and C intervals. The shown upper limits are at 2σ level. For the C interval, the BKNPL model assuming $\Gamma_\gamma = 2.1$ is shown (see Table 1).

3.2. Afterglow emission

The entire observation of 165 ks duration was split into two parts, one of 49.4 ks duration during which the source was visible and fading, and the other of 115.6 ks duration, during which the source was no more visible. The afterglow spectrum of the first part is shown in Fig. 4. Given that below 1 keV the source was detected only marginally, the 2σ upper limit is shown. The spectrum is well fit with a photoelectrically absorbed power–law with Galactic column density $N_{\rm H}^{\rm G}$ and photon index $\Gamma = 1.3^{+0.8}_{-0.6}$. No evidence of spectral evolution with time was noticed. Assuming the best fit spectrum, we derived a 3σ upper limit of 9×10^{-14} erg cm^{-2} s^{-1} to the 2–10 keV

Table 1. Best-fit parameters of the GRB010214 time-averaged spectrum and of its temporal evolution (see text for the definition of slices A, B and C). Errors are at 90% confidence level.

Slice	Duration (s)	Model([a])	$N_{\rm H}$([b])	Γ_X	Γ_γ	$E_{\rm p}$ (keV)([c])	χ^2/ν
A+B+C	28	BKNPL	[0.0266]	$0.86^{+0.13}_{-0.17}$	$2.4^{+0.3}_{-0.2}$	67^{+20}_{-15}	11.7/16
		BL	[0.0266]	$0.65^{+0.16}_{-0.19}$	[2.4]	102^{+42}_{-29}	14.0/17
A	6	PL	30^{+51}_{-20}	1.6 ± 0.2	–	>700	4.66/4
		BKNPL	[0.0266]	$0.34^{+0.43}_{-0.50}$	$2.5^{+0.8}_{-0.9}$	41^{+39}_{-25}	0.86/3
B	8	BKNPL	[0.0266]	$0.91^{+0.15}_{-0.15}$	>1.8	75^{+105}_{-37}	1.8/7
		BL	[0.0266]	$0.73^{+0.24}_{-0.27}$	>1.7	122^{+113}_{-46}	2.6/7
C	14	BKNPL	[0.0266]	[0.81]	>1.9	10^{+9}_{-6}	3.8/2

([a]) PL = power–law; BKNPL = broken power–law. BL = smoothly broken power–law (Band et al. 1993).
([b]) Units of 10^{22} cm^{-2}.
([c]) Peak energy of the $EF(E)$ spectrum.

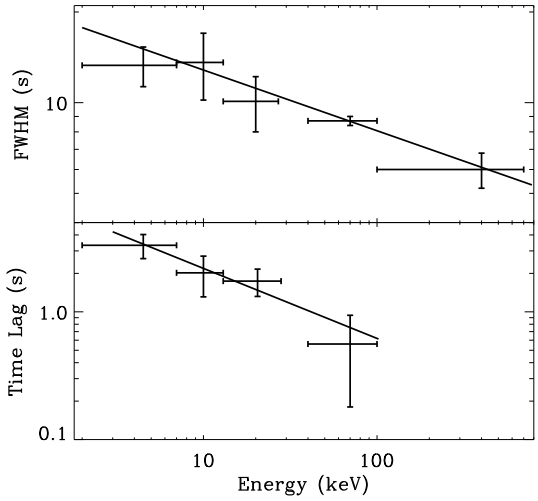

Fig. 3. *Top panel:* pulse *FWHM* as a function of energy with superposed the best power–law fit. *Bottom panel:* lag of the pulse centroid with respect to that in the 100–700 keV band as a function of energy, with superposed the power–law best fit.

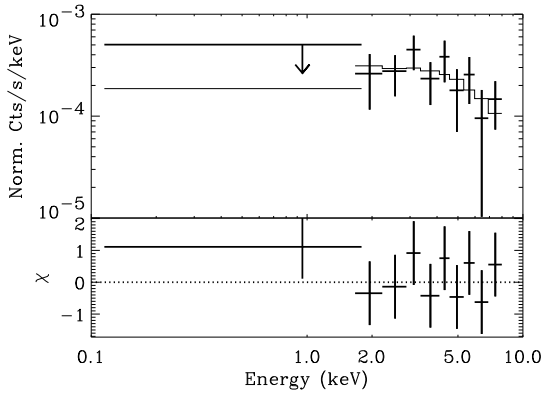

Fig. 4. LECS+MECS23 spectrum of the X–ray afterglow. The best power–law ($\Gamma = 1.3$) fit is shown. The 2-σ upper limit comes from the LECS. In the bottom panel, the residual in correspondence of the LECS upper limit is the measured value in the LECS.

source flux during the second part of the observation (starting at 72 ks after the main event).

Figure 5 shows the 2–10 keV flux decay from the prompt emission (WFC data) to the afterglow (MECS2+3), where the time origin is the GRB onset. Using a power–law model for the decay law ($F_X \propto t^{-\delta}$), the NFI afterglow measurements are well fit with an index $\delta = 2.1^{+1.0}_{-0.6}$. If we include in the fit the last significant point of the prompt emission, we obtain an index $\delta = 1.27 \pm 0.04$, which however is not consistent with the 3σ upper limit provided by the WFC from 30 s to 300 s after the GRB onset. Limiting the light curve analysis from the last significant WFC data point to the second WFC upper limit, the flux decay is consistent with a power–law with slope >1.9, which however is not consistent with the late afterglow data points. This would imply the presence of a bump in the time interval from 300 s to $\sim 3 \times 10^4$ s after the GRB onset.

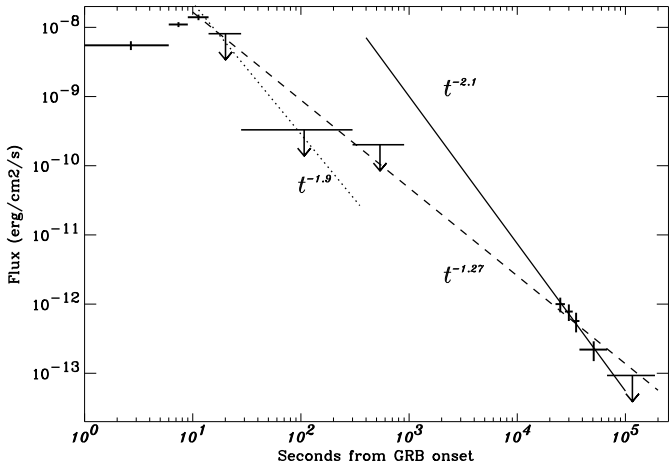

Fig. 5. 2–10 keV flux decay from the prompt emission, assuming as origin the GRB onset. The dotted line indicates the minimum power–law decay slope on the basis of the WFC upper limits; the dashed line is the best-fit power–law decay of the last significant WFC data point and the NFI data; the solid line shows the best fit power–law when only the afterglow measurements are taken into account.

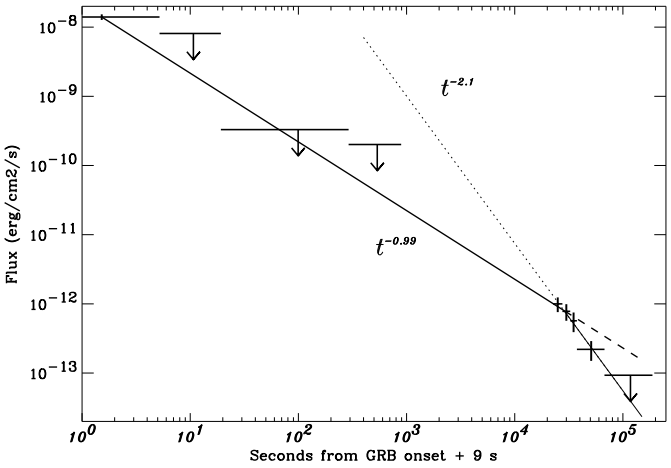

Fig. 6. 2–10 keV flux decay, assuming as origin the GRB onset time plus 9 s. The dashed line indicates the best-fit power–law, obtained by including significant data points from both prompt and afterglow emissions, but the last one. The solid line refers to the best-fit broken power–law.

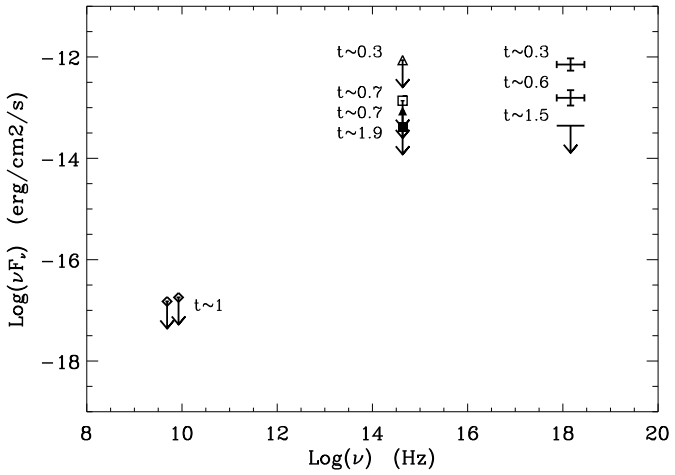

Fig. 7. Afterglow Spectral Energy Distribution: all available upper limits are shown after correction for the Galactic extinction. *open triangle*: Uemura et al. (2001); *open square*: Klose et al. (2001a); *filled triangle*: Hudec et al. (2001); *filled square*: Gorosabel et al. (2001a). The radio upper limits are reported by Berger & Frail (2001). Times are expressed in days.

Alternatively, taking as time origin that corresponding to 9 s after the GRB onset, we obtain the decay curve shown in Fig. 6. This time origin corresponds to ∼50% of the entire time duration of the GRB, where the afterglow is expected to start (Frontera et al. 2000).

If we fit all the significant data points with a single power–law (best fit index $\delta = 1.2$), the WFC upper limits are fulfilled, but the NFI upper limit is not consistent with this best fit curve. This suggests that a break somewhere in the light curve should have occurred. If δ_1 and δ_2 are the power–law indices before and after the break time t_b, respectively, an estimate of δ_2 is $2.1^{+1.0}_{-0.6}$; for δ_1 we fit the same points but the last significant one, since the break time seems to occur somewhat earlier: it comes out $\delta_1 = 0.99^{+0.04}_{-0.09}$, where the shallowest decay allowed (0.90) has been estimated by connecting the WFC point with the WFC 3σ upper limit from 30 s to 300 s; this solution fulfills all WFC and NFI upper limits. An estimate of the break time t_b has been derived by intersecting the two power–laws with their uncertainties. The result is $t_b = 2.9^{+0.7}_{-2.4} \times 10^4$ s, (see Fig. 6).

Figure 7 shows the Spectral Energy Distribution (SED) of the GRB afterglow. In addition to the NFI measurements at different times, all the most sensitive optical, IR and radio upper limits have been shown. The upper limits have been corrected for the Galactic absorption using the color excess $E(B-V) = 0.024$ along the GRB direction (Schlegel et al. 1998), which implies an extinction $A_V = 0.07$ by using the relationship $R_V = A_V/E(B-V) = 3.09 \pm 0.03$ by Rieke & Lebofsky (1985). Following Cardelli et al. (1989) the extinction in the other optical colours is: $A_U = 0.13$, $A_B = 0.10$, $A_R = 0.06$, $A_I = 0.05$, $A_J = 0.02$, $A_K = 0.01$. The corrected magnitudes have been converted into flux densities F_ν (erg cm^{-2} s^{-1} Hz^{-1}) according to the calibration reported by Fukugita et al. (1995).

4. Discussion

From the average spectral hardness, GRB010214 is a classical long GRB. The spectral evolution of the prompt X–ray emission (hard–to–soft) is that typical of GRBs (e.g., Frontera et al. 2000), if, as above discussed, we assume a photoelectrically absorbed PL as the best model for the interval A (see Table 1). Also the power–law dependence of the GRB pulse width on energy above 7 keV is in agreement with similar investigations performed above 10 keV with the BATSE experiment (Fenimore et al. 1995; Norris et al. 1996). The power–law index of the pulse width behaviour with energy ($\alpha_{FWHM} = 0.28 \pm 0.13$) appears consistent with the range of values (0.37 to 0.46) found by Fenimore et al. (1995) and Norris et al. (1996) for a sample of bright BATSE bursts. It is however significantly lower than the corresponding power–law indices found by Feroci et al. (2001) for the X–ray richest GRB990704 (∼0.45) and by Piro et al. (1998a) for GRB960720 (∼0.46). Our result confirms the validity of the working scheme discussed by Norris et al. (1996) that pulses are the basic units in bursts. A peculiarity however emerges below 7 keV: the pulse width shortens while a secondary pulse rises; only the superposition of both pulses gives a $FWHM$ consistent with the extrapolation of the pulse width behaviour at higher energies (see Fig. 3).

A much more peculiar feature of GRB010214 is the possible evidence of variable absorption of the promptly emitted X–ray radiation, from $N_H = 3.0^{+5.1}_{-2.0} \times 10^{23}$ cm^{-2} during the first 6 s of the event down to a value consistent with the Galactic absorption ($N_H^G = 2.66 \times 10^{20}$ cm^{-2}) along the GRB direction. So far, this feature has been observed only for GRB980329 (Frontera et al. 2000), GRB990705 (Amati et al. 2000) and GRB010222 (In 't Zand et al. 2001). As discussed by Lazzati & Perna (2002), variable absorption might be the signature around the burst of an overdense cloud of radius $R < 5$ pc and density $n > 10^3$ cm^{-3}, similar to star formation globules within molecular clouds (Bok globules). The true N_H at the GRB site could be determined only from the knowledge of the GRB redshift z. A tentative estimate of z could be obtained as follows. Amati et al. (2002), analyzing the redshift-corrected average spectra of a sample of 12 *BeppoSAX* GRBs with known

redshift, found a correlation between low-energy photon index Γ_X and redshift z and between isotropic gamma–ray energy $E_{\rm iso}$ (evaluated in the 1–10^4 keV band) and peak energy $E_{\rm p}^{\rm rest}$ in the GRB rest frame. Using the average value of $\Gamma_X = 0.65^{+0.16}_{-0.19}$ (see Table 1) and inverting the relationship found by Amati et al. (2002) ($\Gamma_X = 2.464(1+z)^{-0.78\pm0.18}$), we get $z = 4.5^{+11}_{-2.3}$. On the basis of this result, the minimum value of $N_{\rm H}$ at the GRB site during the time interval A would be about 1×10^{24} cm^{-2}. However, the estimate of z and thus of $N_{\rm H}$ are clearly tentative, since the GRB sample used by Amati et al. to derive their correlation, is still small and should be confirmed by larger GRB samples. The analysis of the afterglow light curve in the 2–10 keV energy band (see Figs. 5 and 6) has shown that either the afterglow starts close to the origin of the main event with the power–law decay near its end, or the afterglow starts after the peak time of the prompt gamma–ray emission. In the former case a bump in the afterglow light curve, something like that found by Piro et al. (1998b) for GRB970508, is inferred; in the latter case a break in the power–law decay should have occurred with an estimated break time of $2.9^{+0.7}_{-2.4} \times 10^4$ s since the GRB onset. Similar breaks in the light curve have been found for GRB990510 (Pian et al. 2001) and GRB010222 (In 't Zand et al. 2001). In these cases it could be established that the breaks are achromatic, given their contemporary presence in the optical band.

Assuming a break, within the fireball model scenario, three different interpretations can be given: 1) deceleration of the fireball into a wind environment (Chevalier & Li 1999, 2000); 2) transition from a relativistic to a Newtonian regime of the outflowing matter (Dai & Lu 1999); 3) deceleration of relativistic ejecta within a jet into a constant density medium (Sari et al. 1999; Rhoads 1999). The mechanism 1) appears unlikely. Indeed, according to the wind model by Chevalier & Li (1999, 2000), assuming a density decrease $\rho(r) \propto r^{-2}$, where r is the distance from the GRB site, when the transition from fast to slow cooling of the expanding fireball takes place, the expected break in the power–law decay index at high frequencies is $\delta_2 - \delta_1 = 1/4$, which does not match the observed break of $1.1^{+1.0}_{-0.6}$. The mechanism 2) appears inconsistent with our data. Indeed, if the steepening of the light curve is due to NRP, for a cooling frequency $\nu_{\rm c} < \nu_{\rm X}$ after the break time, the expected power–law decay index is $\delta_2 = (3p-4)/2$ and the photon index of the PL spectral model is $\Gamma = p/2+1$, where p is the PL index of the electron energy distribution. From the estimate of δ_2 we get $p = 2.7^{+0.7}_{-0.4}$, that would imply an expected value of photon index $\Gamma_{\rm exp} = 2.4^{+0.3}_{-0.2}$ which is inconsistent with the measured value $\Gamma = 1.3^{+0.8}_{-0.6}$. Also in the case $\nu_{\rm c} > \nu_{\rm X}$, this model is still incompatible with our data. Indeed, the power–law decay indices before and after the break time are $\delta_1 = 3(p-1)/4$ and $\delta_2 = (15p-21)/10$, respectively: thus, it is possible to estimate p from the measure of $\Delta\delta = \delta_2 - \delta_1 = 3/4p - 27/20$, and it comes out $p = 3.3^{+1.3}_{-0.8}$. Replacing this value in the expressions of $\Gamma = (p+1)/2$, δ_1 and δ_2, the following estimates are obtained, respectively: $\Gamma_{\rm exp} = 2.15^{+0.65}_{-0.4}$, $\delta_{1\rm exp} = 1.7^{+1.0}_{-0.6}$ and $\delta_{2\rm exp} = 2.8^{+1.2}_{-0.9}$. $\Gamma_{\rm exp}$ and $\delta_{2\rm exp}$ are only marginally compatible with the corresponding measured values, while $\delta_{1\rm exp}$ is incompatible.

The model 3) accounts for the observed properties of the X–ray afterglow, independently whether $\nu_{\rm c} < \nu_{\rm X}$ or $\nu_{\rm c} > \nu_{\rm X}$. Indeed, according to this model, after the break, the expected $\delta_2 = p$ independently of the cooling frequency position in the spectrum and $\Gamma = p/2+1$ if $\nu_{\rm X} > \nu_{\rm c}$, while $\Gamma = p/2+1/2$, if $\nu_{\rm X} < \nu_{\rm c}$. From the estimated value of $\delta_2 = 2.1^{+1.0}_{-0.6}$, $\Gamma_{\rm exp} = 2.0^{+0.5}_{-0.3}$ or $= 1.5^{+0.5}_{-0.3}$, respectively, which are both consistent with the observed index $\Gamma = 1.3^{+0.8}_{-0.6}$. With the found value of $p = 2.1^{+1.0}_{-0.6}$, also the expected index of the decay law before the break δ_1 ($= (3p-2)/4$ if $\nu_{\rm X} > \nu_{\rm c}$, otherwise $= (3p-1)/4$) is consistent with the observations, independently whether $\nu_{\rm c} < \nu_{\rm X}$ or $\nu_{\rm c} > \nu_{\rm X}$.

The assumption of a cooling frequency $\nu_{\rm c}$ below the X-ray band is preferred on the basis of the derived SED (see Fig. 7). Actually, if a high optical extinction is at the origin of the non–detection of the OT (other possible interpretations of the GRB darkness will be considered below), the true SED should rise the optical data points above the X–ray intensities.

Alternatively, if a bump after an initial decay of the X-ray afterglow is assumed (see Fig. 5), the contemporary non–detection of an OT is expected in the case in which the GRB occurs in a dense star–forming region and the afterglow is dominated, minutes to day from the main event, by small–angle scattering off dust grains (Mészáros & Gruzinov 2000). According to this model, the initial afterglow light curve would be that unscattered, while a steeper decay curve is expected after the bump. We observe a similar picture, but the initial light curve is much steeper ($\delta > 1.9$) than the mean steepness of the afterglow light curves ($< \delta >= 1.30 \pm 0.02$) (Frontera 2002). In addition an IR counterpart, expected to be detected from such dark events at several days distance from the main event has not been reported. Thus, even though this model cannot be ruled out, the break hypothesis and its interpretation in terms of a spreading jet model appears more likely.

An open question is the density of the circumburst medium. At the onset of the main event it is likely to be high as confirmed by the initial absorption of the prompt X–ray emission. However the late prompt emission and afterglow spectra are consistent with a Galactic column density. Likely the GRB released energy has almost completely ionized the initially absorbing cloud (Lazzati & Perna 2002). In this scheme however we would expect to see the optical counterpart, as in the case of GRB980329 (Palazzi et al. 1998), which also showed an initial high absorption (Frontera et al. 2000), and even a column density a factor 10 higher than the Galactic one during the afterglow phase (In 't Zand et al. 1998). Thus a likely explanation of the GRB010214 darkness could reside in an intrinsic faintness of the related OT and/or the high GRB redshift (centroid value of 4.5) estimated by us. The non-detection of a radio counterpart of GRB010214 might also be related to an intrinsic faintness of the source.

An important question in this respect is whether the non-detection of the OT is due to low sensitivity searches. To solve this issue, we have compared the published optical upper limits of GRB010214 with those of other dark GRBs and with the optical light curves of faint OTs. In Fig. 8 we show the result, adapted from Fig. 3 of the paper by Fynbo et al. (2001). Also shown is the best fit curve, obtained by Lazzati et al. (2002)

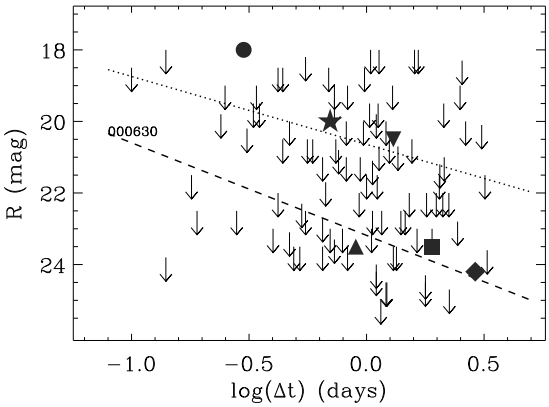

Fig. 8. Limiting *R*-band magnitudes vs. observation times for 55 GRBs without optical afterglow detection. The dotted line shows the best linear fit obtained by Lazzati et al. (2002) between *R* magnitude and detection time for a sample of detected optical afterglows. The dashed line shows the power–law decay of the OT of GRB000630 (Fynbo et al. 2001), one of the faintest OTs within 1 day from the GRB. The filled symbols refer to the following upper limits for GRB010214: the circle comes from Uemura et al. (2001), the star from Klose et al. (2001a), the triangle and the diamond from Rol et al. (2001b), the upside down triangle from Hudec et al. (2001), the square from Masetti et al. (2001b). Adapted from Fynbo et al. (2001).

for a sample of GRBs, which expresses the *R* magnitude as a function of the detection time. The reported GRB010214 upper limits do not seem to suffer from inadequate sensitivity observations when compared with other bursts.

5. Conclusions

GRB010214 is a classical, long burst with detected X–ray afterglow, but dark in the optical and radio band, despite sensitive and prompt searches.

The prompt emission shows the typical hard-to-soft spectral evolution with a possible high column density ($N_{\rm H} = 3.0^{+5.1}_{-2.0} \times 10^{23}$ cm^{-2}) in excess of the Galactic one ($N_{\rm H}^{\rm G} = 2.66 \times 10^{20}$ cm^{-2}) along its direction in the first 6 s. Other three bursts were found to show similar variable absorptions: GRB980329 (Frontera et al. 2000), GRB990705 (Amati et al. 2000) and GRB010222 (In 't Zand et al. 2001). Using the correlation between low-energy photon index of the prompt emission and redshift found by Amati et al. (2002), we have tentatively estimated the redshift $z \sim 4.5$ of GRB010214.

The 2–10 keV afterglow light curve suggests the presence of a steepening or a bump before the NFI observation with a break time of $2.9^{+0.7}_{-2.4} \times 10^4$ s from the GRB onset. The model which appears to better fit the data is a spreading jet in either a typical ISM or in an overdense ionized cloud. The latter environment is more likely, given the initially high $N_{\rm H}$. In the jet scenario, the power–law index of the electron energy distribution has been derived ($p = 2.1^{+1.0}_{-0.6}$) and it is inside the range of values found for a sample of *BeppoSAX* GRBs (Frontera et al. 2000).

Acknowledgements. This research is supported by the Italian Space Agency (ASI) and Ministry of University and Scientific Research of Italy (COFIN funds). We wish to thank the Mission Director L. Salotti and the teams of the *BeppoSAX* Operation Control Center, Science Operation Center and Scientific Data Center for their efficient and enthusiastic support to the GRB alert program.

References

Amati, L., Frontera, F., Vietri, M., et al. 2000, Science, 290, 953
Amati, L., Frontera, F., Tavani, M., et al. 2002, A&A, 390, 81
Anders, E., & Ebihara, M. 1982, Geochim Cosmochim. Acta, 46, 2363
Antonelli, L. A., D'Alessio, F., & Di Paola, A. 2001, GCN Circ., 944
Arnaud, K. A. 1996, in Astronomical Data Analysis Software and Systems V, ed. J. Jacoby, & J. Barnes, ASP Conf. Ser., 101, 17
Band, D., Matteson, J., Ford, L., et al. 1993, ApJ, 413, 281
Berger, E., & Frail, D. A. 2001, GCN Circ., 943
Boella, G., Butler, R. C., Perola, G. C., et al. 1997, A&AS, 122, 299
Cardelli, J. A., Clayton, G. C., & Mathis, J. S. 1989, ApJ, 345, 245
Chevalier, R. A., & Li, Z. Y. 1999, ApJ, 520, L59
Chevalier, R. A., & Li, Z. Y. 2000, ApJ, 536, 195
Cowsik, R. 2001, GCN Circ., 978
Dai, Z. G., & Lu, T. 1999, ApJ, 519, L155
Di Paola, A., D'Alessio, F., & Antonelli, L. A. 2001, GCN Circ., 939
Djorgovski, S. G., Kulkarni, S. R., Bloom, J. S., et al. 2001, in Proc. Gamma-Ray Bursts in the Afterglow Era: 2nd Workshop, ed. E. Costa, F. Frontera, & J. Hjorth, ESO Astrophysics Symposia, 218
Fenimore, E. E., In 't Zand, J. J. M., Norris, J. P., Bonnell, J. T., & Nemiroff, R. J. 1995, ApJ, 448, L101
Feroci, M., Antonelli, L. A., Soffitta, P., et al. 2001, A&A, 378, 441
Frontera, F., Costa, E., Dal Fiume, D., et al. 1997, A&AS, 122, 357
Frontera, F., Amati, L., Costa, E., et al. 2000, ApJS, 127, 59
Frontera, F., Guidorzi, C., Antonelli, L. A., et al. 2001, GCN Circ., 950
Frontera, F. 2002, in Supernovae and Gamma Ray Bursts, ed. K. Weiler (Berlin, Springer & Verlag), in press
Fruchter, A. 1999, ApJ, 512, L1
Fukugita, M., Shimasaku, K., & Ichikawa, T. 1995, PASP, 107, 945
Fynbo, J. U., Jensen, B. L., Gorosabel, J., et al. 2001, A&A, 369, 373
Galama, T. J., Wijers, R. A. M. J., Bremer, M., et al. 1998, ApJ, 500, L97
Gandolfi, G. 2001, GCN Circ., 933
Gorosabel, J., Fynbo, J. U., Jensen, B. L. J., et al. 2001a, GCN Circ., 949
Gorosabel, J., Fynbo, J. U., Jensen, B. L., et al. 2001b, GCN Circ., 972
Guidorzi, C., Frontera, F., Gennaro, G., et al. 2001, GCN Circ., 951
Harrison, F. A., Bloom, J. S., Frail, D. A., et al. 1999, ApJ, 523, L121
Harrison, F. A., Yost, S. A., Sari, R., et al. 2001, ApJ, 559, 123
Henden, A. 2001, GCN Circ., 988
Hudec, R., Jelinek, M., Tichy, M., & Ticha, J. 2001, GCN Circ., 942
In 't Zand, J. J. M., Amati, L., Antonelli, L. A., et al. 1998, ApJ, 505, L119
In 't Zand, J. J. M., Kuiper, L., Amati, L., et al. 2001, ApJ, 559, 710
Jager, R., Mels, W. A., Brinkman, A. C., et al. 1997, A&AS, 125, 557
Klose, S., Stecklum, B., Castro-Tirado, A., & Greiner, J. 2001a, GCN Circ., 935
Klose, S., Stecklum, B., Linz, H., & Laux, U. 2001b, GCN Circ., 997
Lazzati, D., & Perna, R. 2002, MNRAS, 330, 383
Lazzati, D., Covino, S., & Ghisellini, G. 2002, MNRAS, 330, 583
Masetti, N., Palazzi, E., Pian, E., et al. 2001a, A&A, 374, 382
Masetti, N., Palazzi, E., Pian, E., et al. 2001b, GCN Circ., 954
Mészáros, P., & Gruzinov, A. 2000, ApJ, 543, L35
Morrison, R., & McCammon, D. 1983, ApJ, 270, 119
Norris, J. P., Nemiroff, R. J., Bonnell, J. T., et al. 1996, ApJ, 459, 393
Palazzi, E., Pian, E., Masetti, N., et al. 1998, A&A, 336, L95

Pian, E., Soffitta, P., Alessi, A., et al. 2001, A&A, 372, 456
Pian, E. 2002, in Supernovae and Gamma Ray Bursts, ed. K. Weiler (Berlin Springer & Verlag), in press
Piran, T. 1999, Phys. Rep., 314, 575
Piran, T. 2000, Phys. Rep., 333, 529
Piro, L., Heise, J., Jager, R., et al. 1998a, A&A, 329, 906
Piro, L., Amati, L., Antonelli, L. A., et al. 1998b, A&A, 331, L41
Piro, L. 2002, Proc. of the 3rd workshop of GRB in the afterglow era (in preparation)
Rhoads, J. E. 1999, ApJ, 525, 737
Rieke, G. H., & Lebofsky, M. 1985, ApJ, 288, 618
Rol, E., Salamanca, I., Kaper, L., Vreeswijk, P., & Tanvir, N. 2001a, GCN Circ., 1059
Rol, E., Salamanca, I., Kaper, et al. 2001b, GCN Circ., 955
Sari, R., Piran, T., & Halpern, J. P. 1999, ApJ, 519, L17
Schlegel, D. J., Finkbeiner, D. P., & Davis, M. 1998, ApJ, 500, 525
Stanek, K. Z., Garnavich, P. M., Kaluzny, J., Pych, W., & Thompson, I. 1999, ApJ, 522, L39
Uemura, M., Kato, T., & Yamaoka, H. 2001, GCN Circ., 948
Wei, D. M., & Lu, T. 2002, MNRAS, 332, 994
Zhu, J., & Xue, S. J. 2001, GCN Circ., 938